New Materials, Compounds and Applications
Vol.6, No.3, 2022, pp.282-293

SUPERHYDROPHOBIC SILICA MONOLITHIC DOPED WITH CRYSTAL VIOLET DYE UNDER AMBIENT PRESSURE: PREPARATION AND CHARACTERIZATION

Samah S. Ahmed, Israa F. Al-Sharuee*

Department of Physics, College of Science, Mustansiriyah University, Baghdad, Iraq

Abstract. This paper prepares and investigates superhydrophobic silica aerogels doped with Crystal Violet dye. The primary contribution is to obtain a product with the best specifications in the shortest amount of time possible. In the preparation, two procedures were used: first, the modification step after the sample is converted to alcogel, known as CV1. Second, CV2 refers to the alteration that occurs prior to conversion to gel (in the sol stage). The spectral, structural, and morphological properties have been exanimated using FTIR, BET, XRD, and FESEM. The improved surface's hydrophobicity is assessed using contact angle measurements. Except for the obvious increase in density, this work shows that Crystal Violet dye can improve the structural properties of silica aerogel. Aerogel has higher specs and greater improvements when n-hexane is mixed with the sol before it transforms into gel than when it is changed after it goes into gel.

Keywords: *silica aerogel, superhydrophobic, dye laser, Crystal Violet, ambient pressure.*

Corresponding Author*: Israa F. Al-Sharuee, Department of Physics, College of Science, Mustansiriyah University, Baghdad, Iraq, Tel.: +9647702787336, e -mail: i81f54@uomustansiriyah.edu.iq*

Received: *18 June 2022;* ***Accepted:*** *12 November 2022;* ***Published:*** *7 December 2022.*

1. Introduction

Silica aerogel is a promising nanomaterial initially created by Dr. Samuel Stephen Kistler in 1930, involving 90% air of its volume, certifying low thermal conductivity (Bi *et al.*, 2013; Xie *et al.*, 2013). Significantly due to its low density and transparency (Feng *et al.*, 2018). aerogel has a wide range of qualities that make it a viable option for the thermal insulation of walls and windows (Cuce *et al.*, 2014). It can be used to decrease heat generation (Błaszczyński *et al*., 2013; Kim & Hyun, 2003; Pan *et al.*, 2017; Yuan *et al.*, 2012). Various processes are used to create nano-particles of silica material, including vapor-phase reactions (Xu *et al.*, 2021), sol-gel, and thermal decomposition (Liou , 2004). Generally, hydrophilic and hydrophobic silica aerogels are prepared through the sol-gel process, mainly producing aerogels (Mohammed & Hussein, 2020). Hydrophobic functional groups are spliced to the aerogel surface employing surface modification (He & Chen, 2017; Li *et al.*, 2016).

Many researchers have studied the heat transfer properties of aerogel materials (He *et al.*, 2019; Yuan *et al.*, 2012). There are many techniques that mainly depend on the production of silica aerogel. The most commonly used are the supercritical drying technique (SCD) and the ambient pressure drying technique (APD) (Karamikamkar *et*

How to cite (APA):
Ahmed, S.S., Al-Sharuee, I.F. (2022). Superhydrophobic silica monolithic doped with Crystal Violet dye under ambient pressure: preparation and characterization. *New Materials, Compounds and Applications, 6*(3), 282-293.

al., 2020; Mazrouei-Sebdani *et al.,* 2021). The APD technique has been relied on as a more desirable and feasible alternative to traditional drying methods (Gupta *et al.,* 2018). Compared to the APD method, supercritical drying is a costlier and potentially dangerous technology. Furthermore, it requires the autoclave to operate at high pressures and temperatures in the presence of organic solvents. These limitations limited the commercial growth of aerogel manufacturing using this technique, which resulted in the switch to the drying process at atmospheric pressure (Oh *et al.,* 2009; Rao *et al.,* 2001). The challenge of APD is how to control the removal of pore liquid from a wet gel without the cussing of shrinkage or the creation of cracks, which can be caused by capillary pressure during the condensation of surface silanol groups (Si-OH) process (Al-Sharuee & Mohammed, 2019; Yun *et al.,* 2014). This method mainly replaces the silanol groups with alkyl groups Si-R to avoid condensation and shrinkage (Nazriati *et al.,* 2014).

Many parameters affect the surface modification of hydrophobic silica aerogel, such as pH, R-molar ratio, temperature, the concentration of silanol, and the doping through the preparation process (Sinkó, 2010). Moreover, it was found that the doping in metal ions can improve the hydrophobicity property by decreasing the (O-H) bonds and replacing them with the bonds of metals (Peterson *et al.,* 2014). Additionally, it was found that the doping in laser dyes gives more improvements in several characterizations of silica aerogel, such as morphological, structural, and the hydrophobicity property (Bhagat & Rao, 2006; Li *et al.,* 2015). This doping achieved a lot of industrial applications (Sciuti *et al.,* 2019). Some researchers succeeded in preparing silica aerogel doped with coumarin dye. They noticed that the interaction of these dyes with silica gel results in excellent uniformity and transparency in the final product (Haque & Husain, 2014). Another study produced doped silica aerogel with Rhodamine (6G) in an ambient pressure method; the study obtained a light-weighted material with (0.28 to 0.17) gm/cm^3, high surface area, and contact angle (AL-Sharuee, 2021). In this work, Crystal Violate is utilized as a doped dye in silica aerogel to investigate the characteristics of connecting and interaction between the silanol groups and dye. Furthermore, it focuses on the dye effect on the product through improvements in the surface area, average pore size and volume, contact angle, and structural properties. Two procedures were depended on to prepare the product in this work. Firstly, the modification process was on the alcogel by adding the dye after the condensation step. The second was to mix the dye with n-hexane before the hydrolysis (this is a modification step) and quickly produce the hydrophobic aerogel.

2. Materials and methods

Tetraethylorthosilicat (TEOS, 98 %) chemical formula Si $(OC_2H_5)_4$ equipped from Sigma-Aldrich, Germany. Trimethylchlorosilane (TMCS, > (98%) chemical formula $(CH_3)_3SiCl$, from TCI Japan. N-hexane (C_6H_{14} > 98%), from CHem-LAB (Belgium). Ethanol absolute from Schariau (Spain) > (99%). Crystal Violet dye chemical formula ($C_{25}N_3H_{30}Cl$) molecular weight 407.979 (g/mol) from SCRC-India. Hydrochloric acid (HCl) (35-38%), from Thoma Baker (India). Ammonia Solution (NH_4OH) from CDH (India). Condensed silica (CS) was made by combining TEOS as a precursor in ethanol and HCl (0.1 M) as an acidic catalyst, with a molar ratio of TEOS to Etho: HCl of (1:5: 0.2). Two procedures are available for the preparation of doped silica aerogel in CV. Firstly, add different amounts of 10^{-2} gm/cm^3 from CV to CS, each

put under a magnetic stirrer for 15 min, then add the base catalysis (0.5M NH_4OH) to convert the sol to the gel. After 15 min, the gel is aged for two hours, and washed in ethanol three times every 24 hrs. The surface modification was made by mixing TMCS and n-hexane at a ratio of 1:6 M under 60ºC for 24 hrs. The residual TMCS was removed from the modified gel by washing it in pure n-hexane for 24 hours twice at room temperature, then wrapping it in plastic covering small holes and letting it dry at ambient pressure. Then it is treated with a gradual temperature of 120ºC every 10ºC to get the hydrophobic silica aerogel doped in CV.

The second procedure, called "CV2," was by adding n-hexane to CS before the doping step, then adding (0.5 and 2) ml of 10^{-2} gm/cm^3 CV dye, then magnetic stirring for 15 min, adding 0.5M NH_4OH, and 5 minutes converted to gel. It aged for 30 min under 50ºC, then was socked in n-hexane for 24 hrs. at 60ºC. The surface modification was made by using TMCS and n-hexane with an additional ratio of (1:6 M) at 60ºC two times every 24 hrs. Then add only the pure n-hexane three times under 60ºC for 24 hours. Lastly, the plastic container was plastic-wrapped with tiny holes and remained dry at ambient pressure for 72 hours. They are treated with a gradual temperature of 120ºC every 10 ºc to get the hydrophobic silica aerogel doped in CV.

The bulk density of doped aerogel was calculated using mass and volume measurements. The volume of the aerogel was estimated using the formula $V = \pi R^2 h$, where R is the radius and h is the height of the aerogel. If "m" denotes the mass of the aerogel, its bulk density equals m/V. The chemical structure and band regions of aerogels were specified by FTIR spectroscopy (Bruker FTIR Spectrometer ALPHA II, USA), in the range of wave number from 400 to 4000 cm^{-1}. The crystallinity determined via X-Ray Diffraction patterns of the materials was studied by (GaliPIX^{3D} X-ray Detector | 2D Hybrid Pixel XRD Detector) using Cu K radiation (1.5406). The N2 gas adsorption-desorption technique and a surface analyzer were used to investigate the aerogels' structure qualities under the BET examination (BELSORP-mini II). The quantity of N_2 gas adsorbed at different partial pressures (0.01p/p01) revealed the specific surface area, pore size distributions, and total pore volume. The Field Emission Scanning Electron Microscopy (FESEM EBSD Instrument: ZEISS SIGMA VP) was used to analyze the aerogels' microstructure. FESEM is performed by Energy Dispersive Spectroscopy (EDS) for the elemental analysis of surfaces. To estimate the aerogels' hydrophobicity, a water drop (3µ) was placed on the top surface of a sample. From the measurement of the height (h) and width (w) of the drop, the contact angle (θ) was calculated according to the equation (1) (Yaghoobi & Fereidoon, 2018):

$$\theta = 2\tan^{-1}\frac{2\,h}{w} \quad . \tag{1}$$

3. Results and discussion

The physical properties of doped silica aerogel are prepared in two procedures with different amounts of dye, shown in Table 1. The difference in the surface area, total pour volume, and mean pour diameter because of the change in dye concentration Also, adding n-hexane to the sol leads to reservation dye within the silica network. The interaction of a polar solvent with the solution of Crystal Violet causes extraordinary changes in the appearance of the solutions. As previously noted, the observed modifications may be explained by the fact that Crystal Violet behaves as an ion-pair in

non-polar solvents such as n-hexane and as a solvated ion in polar solvents such as ethanol, methanol, etc. The behavior of dye in non-polar solutions implies that the solvent interaction around the dye cation is diminishing due to increasing self-association of the solvent molecules (Korppi-Tommola & Yip, 1981). Resulting in decreasing the surface area, pour volume, and average pour dimeter. In the case of the first method, there is a washing in ethanol. This wash causes more dye loss, resulting in a lower concentration than before; this indicates that dye is not saved in the inner structure of silica aerogel, as evidenced by density values.

Table 1. Some of the physical properties of silica aerogel doped with Crystal Violet

Type of samples	Amount of dye (ml)	Surface area(m^2/g)	Mean pore diameter (nm)	Total pore volume (cm^3/g)	V_m (cm^3/g)	Average Particle size nm	Density g/cm^3	Contact angle θ
CV1	0.5	944	3.5	4.4	204	29.76	0.247	151.75
	1	935	4.1	3.1	188	33.09	0.272	143.36
	1.5	920	4.9	2.90	200	38.62	0.284	147.98
	2	903	12.138	2.742	207	45.49	0.258	145.58
CV2	0.5	970	13.93	3.37	222	42.87	0.087	153.18
	2	754	5.653	1.066	173	53.35	0.135	146.72

FTIR analysis

FTIR analysis for two types of doped silica aerogels, CV1 and CV2, is illustrated in figures 1 (a and b). In all samples, there are noticeable strong peaks at 1313 cm^{-1} and 460 cm^{-1} due to Si–O–Si bands (Han *et al.*, 2015). As the dye concentration rises, this trough becomes less visible. The bending stretching of Si-CH_3 was seen in the peaks at 3285, 1588, and 1013 cm^{-1}. At the same time, the peaks assigned to the H-OH lie at 3556 and 1690 cm^{-1}. Furthermore, the peak attributed to the Si-OH at 1160 $cm^{-}1$ is significantly reduced with the subsequent alteration of TMCS/n-hexane, as shown in the figures. Because of the high effect of a modified solution, the hydrophobic groups (alkyl) replaced the hydrophilic ones (silanol groups). This peak becomes weaker when increasing dye concentration, as shown in the figure, leading to the success of the modification of TMCS/n-hexane, and surface modification was almost completed (Al-Sharuee, 2019; Berardi & Zaidi, 2019). Other peaks were observed at 3556 and 1690 cm^{-1} and were attributed to H-OH bands which were much reduced, to the point that the Si-OH 1160 cm^{-1} peak was no longer noticeable (Linhares *et al.*, 2019). With the comparison between the two figures, it can be said that the addition of n-hexane to the sol before converting to gel Fig. 1(b), plays an important role in modifying the silica surface and, with low concentration, improves the hydrophobicity property as shown in contact angle values.

The intensities of bands O-H, C-H, Si-C, and Si-O-Si for the two samples (CV1) and (CV2) from the FTIR spectrum are illustrated in table 2. The higher transmitted point in these spectra is signed as the (max) mark. The Si-OH is gradually increased by increasing the amount of dye. This indicates more modifications and more replacements in alkyl groups. This is supported through an increased contact angle.

X-Ray diffraction

Fig. 2 (a, b) illustrates the X-Ray diffraction of silica doped in Crystal Violet in different ways, with CV1 and CV2 having the same amount of addition (2 ml). Amorphous silica is responsible for a very large diffraction hump on the XRD graph of composite material, extending from 2θ equal to 12° to 26° on the composite material. Another strong peak is detected at 2θ = 2.4°, which corresponds to the mesoporous characteristic of the material and is measured. An organized structure of mesoporous material was proven using small-angle XRD patterns and conspicuous diffraction peaks (Hrubesh). These results indicate that the produced samples are characterized by high transparency, allowing the passage of significant amounts of light due to the large quantities of silica that make them up.

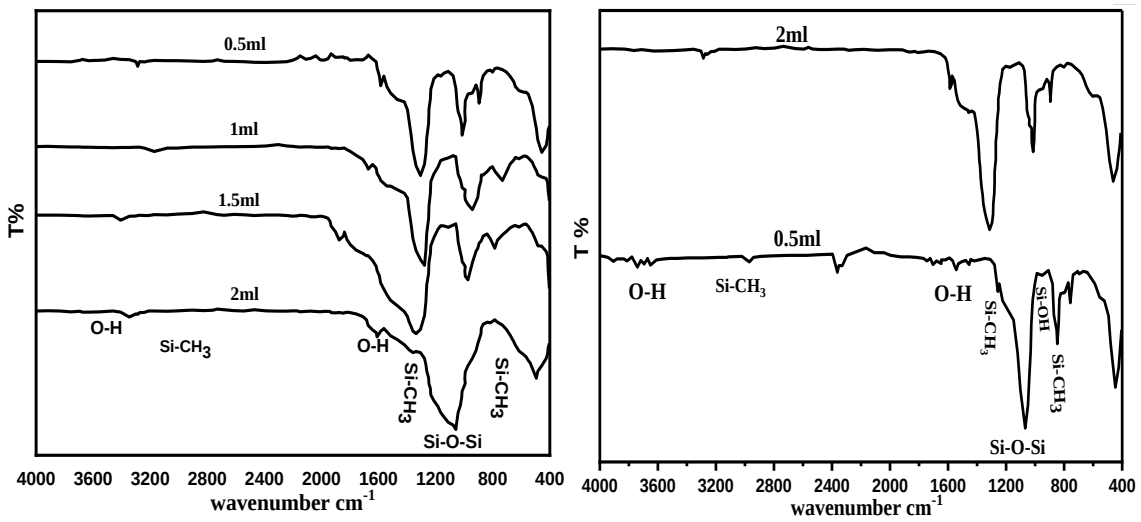

(a) CV1 (b) CV2

Fig. 1. FTIR spectrum for silica aerogel prepared in different procedures

Table 2. Characteristic intensities in FTIR spectra

Name	Amount of dye (ml)	length	OH	CH	Si-CH	Si-OH
CV1	0.5	78.2	0.7	4.5	17.5	28.4
	1	80.1	0.5	3.3	15.1	26.6
	1.5	80	0.3	3.4	16.8	27.4
	2	80	0.8	4.1	17.5	28.1
CV2	0.5	76.1	2	2.5	15.5	28
	2	75	1.3	2	24	32

FESEM and EDS analysis

Fig. 3 (a, b) showed the microstructure of the two samples, CV1, and CV2 (for the two samples, the amount of added dye to the sol was 2 mL) by Field Emission Scanning Electron Microscopy (FESEM) images. At different magnifications, the silica aerogel

exhibited a pearl chain or small ball morphology with a three-dimensional network that was constructed by nanometer-sized silica particles. It observed a smooth surface with no aggregations, besides at the same magnification. It was noted that the average particle size in the case of the addition of n-hexane (CV2) was bigger than when it was added after being converted to gel; this was returned to be the molecular dye in the silica network. On the other hand, the dye is soluble in non-polar or slightly polar organic solvents. Furthermore, there is no evidence of microstructural inhomogeneous from the two ways of preparation, such as significant inter-granular pores between the silica particles. This means that the doped silica aerogel in Crystal Violet does not negatively affect its homogeneous properties.

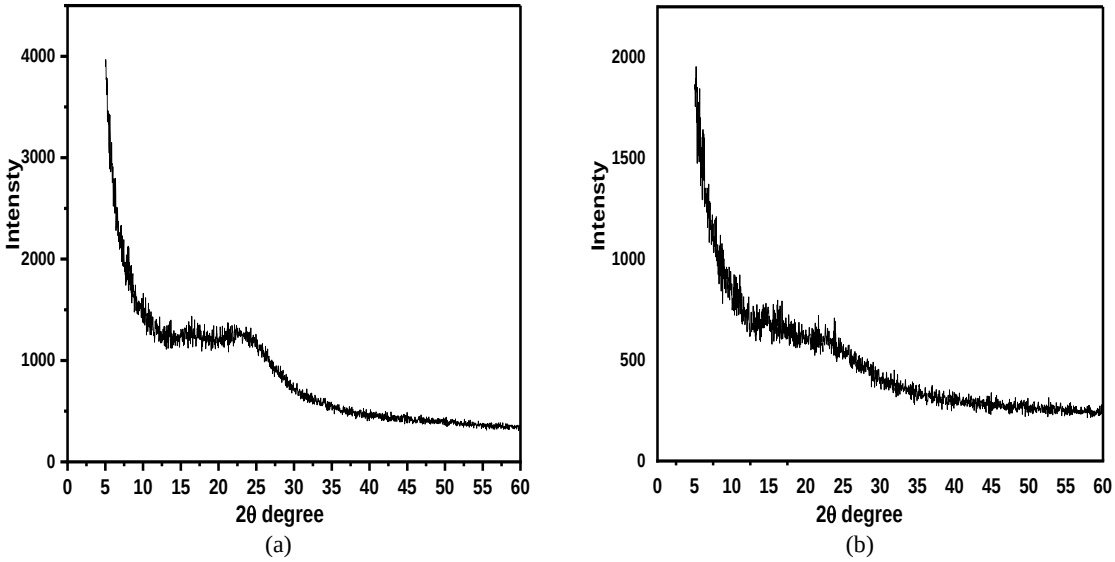

Fig. 2. XRD silica doped in Crystal Violet (a) CV1(b) CV2

The elemental analysis of surfaces in SEM is performed using EDS. The qualitative analysis of Si, O, C, and Cl for CV1 and CV2 samples is observed as illustrated in Figs. 4 (a, b). The detection limit in EDS depends on sample surface conditions; the smoother the surface, the lower the detection limit. Relatively, there is a lot of Si, O, and C in the structure of doped silica aerogel when n-hexane is added to the sol in the condensation step, compared to when the addition is converted to gel in the alcogel step. At the same time, the same amount of Cl is noticed in both cases. In the case of CV1, washing in ethanol plays an essential role in reducing these amounts, except when there is no effect. In contrast, in the case of CV2, a lot of the mentioned quantities remain within the silica network. They will appear in the Dynamic Light Scattering analysis.

Nitrogen adsorption-desorption diagram (BET)

The isotherm of N2 adsorption-desorption of the aerogels of the two samples, CV1 and CV2, (for the two samples, the amount of added dye was 2ml only for the CV1 sample, and 0.5 and 2ml for the CV2 samples) is shown in Fig.5 (a, b, and c), respectively. All aerogel samples exhibited a typical Type II adsorption-desorption isotherm, indicating that the aerogels produced in this investigation are mesoporous (Li *et al*., 2002; Shi *et al*., 2006). The isotherm of a doped aerogel type (CV2), generated

with n-hexane added to the silica sol, is identical to that of a control aerogel synthesized compared with (CV1). The hysteresis loop can be seen in both the aerogel samples (a) and (b) figures. It has cylindrical pores in its structure, which makes it show a unique H2(b) hysteresis loop. complexity of pore structures, in which network effects are significant. When it comes to the type H2 (b) loop, it is related to the pore-blocking return to doping in the dye, but the size range of neck widths is much more significant. Following that hydrothermal treatment, the hysteresis loop of this type has been seen in monocellular silica foams, and some mesoporous ordered silica, among other materials.

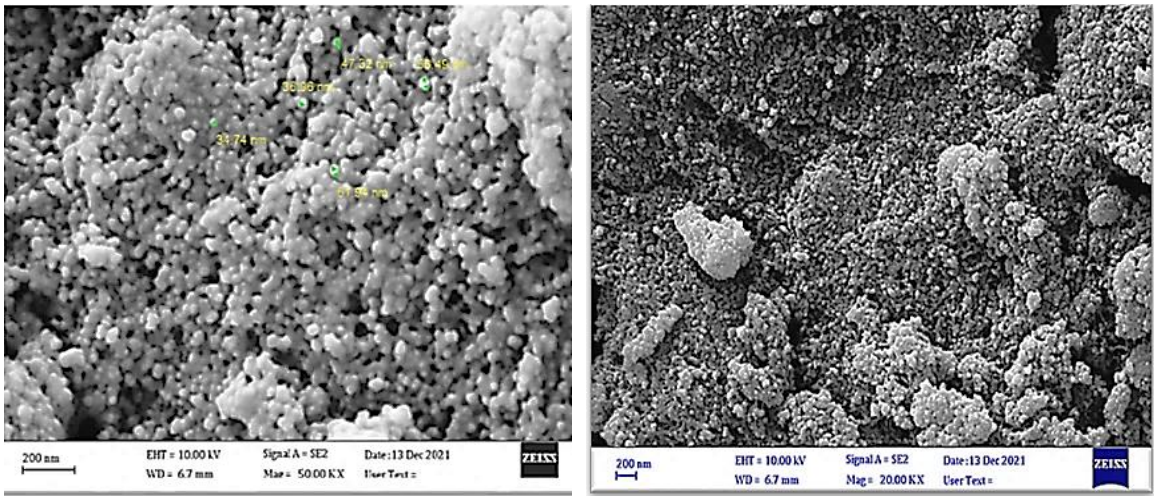

(a) FESEM image for CV1

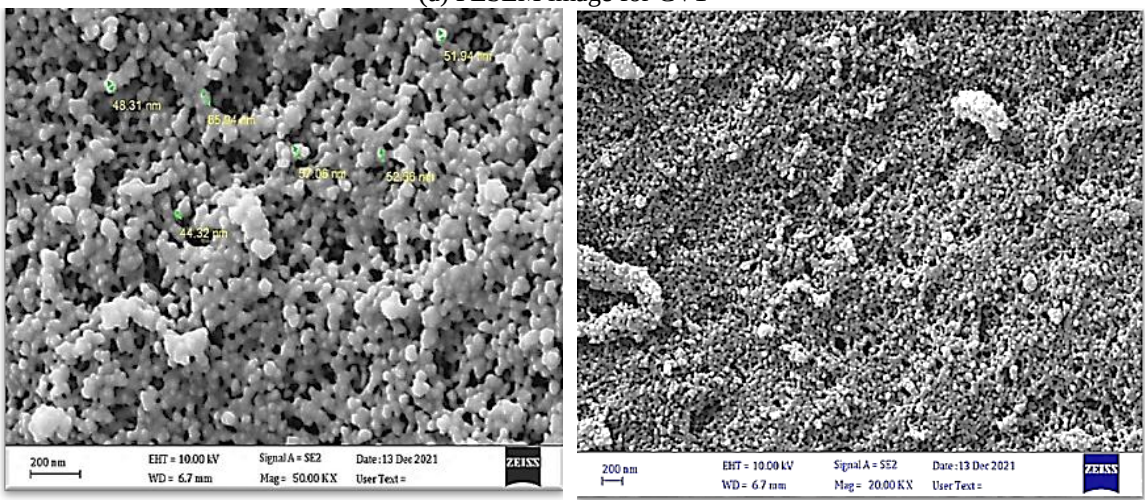

(b) FESEM image for CV2

Fig. 3. FESEM image for the sample of aerogel doped with (a) CV1 (b) CV2

The pore volume of the aerogel type (CV1) from BET was examined, and the hysteresis loop was compressed. A distinction between pores was shown to be responsible for the change in adsorption isotherms seen with age. In Fig. 5(c), the hysteresis loop was of the H3 type, with open cylindrical mesopores that showed adsorption hysteresis. The following two characteristics distinguish the Type H3 loop: I. The adsorption branch is similar in shape and behavior to a Type II isotherm. The lower limit of the desorption branch is generally located near the cavitation-induced adsorption branch. These loops are produced by non-rigid aggregates of plate-like particles (for example, some clays),

but they may also be produced if the pore network is composed of macropores that have not been filled with pore condensate. (Štengl *et al.*, 2006).

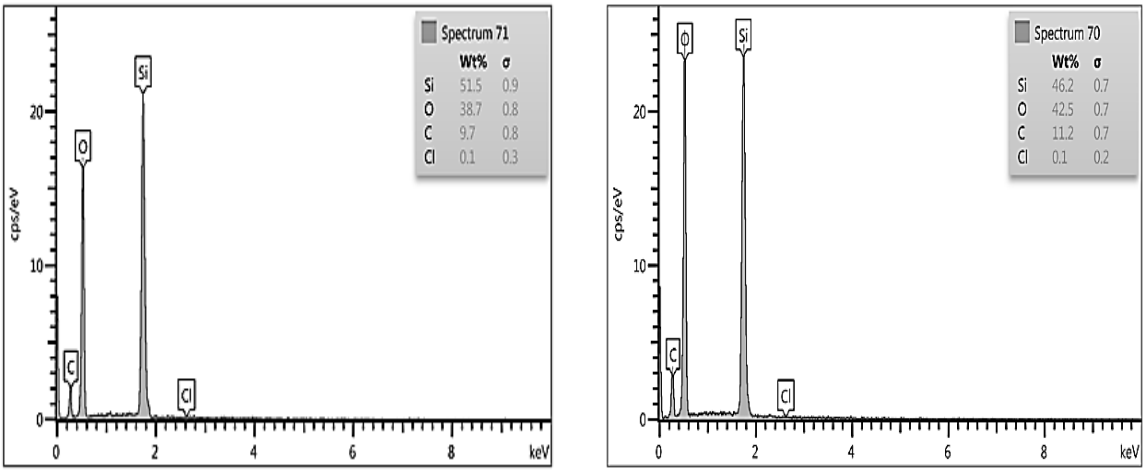

(a) (b)

Fig. 4. EDS analysis for (a) CV1 (b) CV2 samples

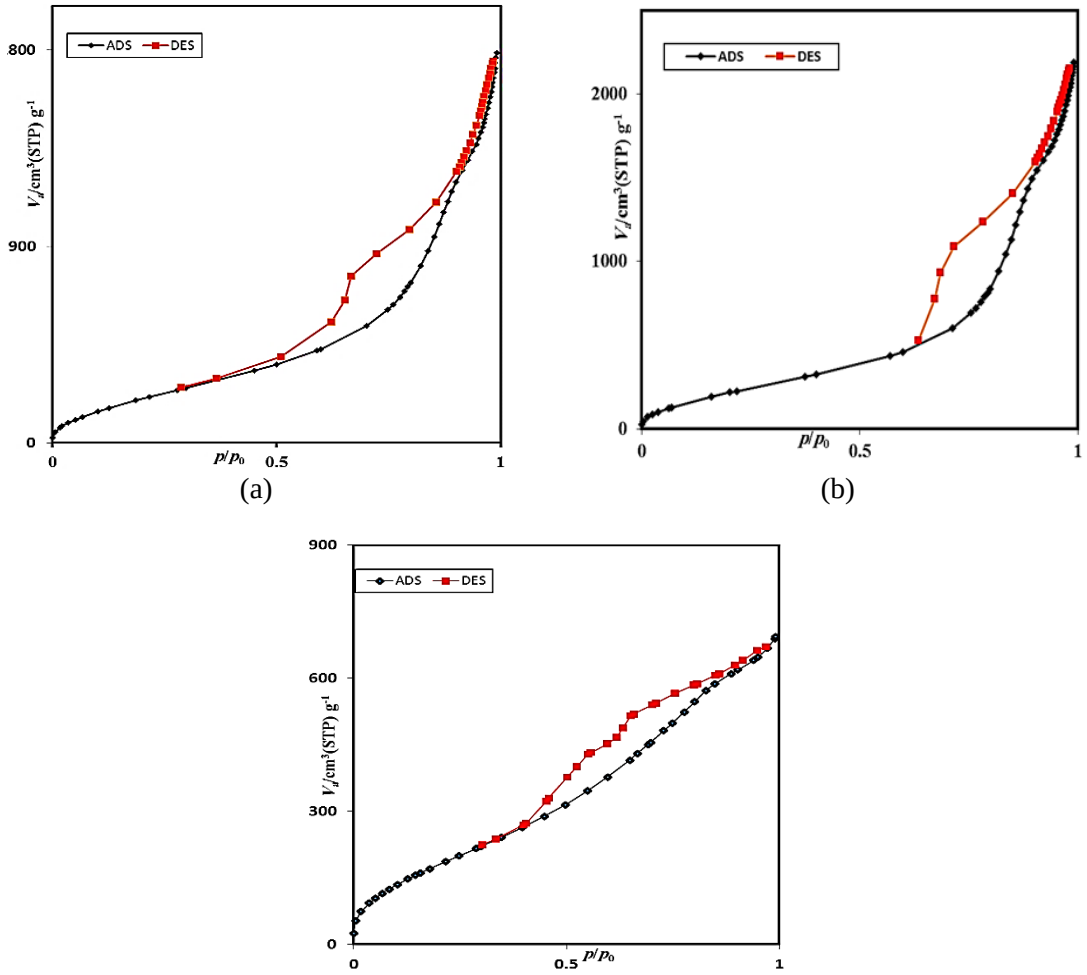

(a) (b)

(c)

Fig. 5. N2 adsorption–desorption isotherms for the doped silica aerogels:
(a) CV1 (b) CV2 0.5 ml (c) CV2 2ml

Contact angle measurement

The quality of the hydrophobic qualities can be determined by measuring the contact angle between a water drop supported on the external surface and the surface under consideration. While maintaining the aerogels in the same environment, it was possible to investigate the influence of doping and the addition of n-hexane on silica sol on the hydrophobicity of the aerogels by measuring the contact angle between the aerogels. The variation in contact angle of the aerogel's samples for CV1 in the amount of dye was (0.5, 1, 1.5, and 2 ml) represented in figures 6 (a, b, c, and d) respectively, whereas the contact angle of the aerogel's samples for CV2 in the amount of dye was (0.5, and 2 ml) represented in Figs. 6 (e, f).

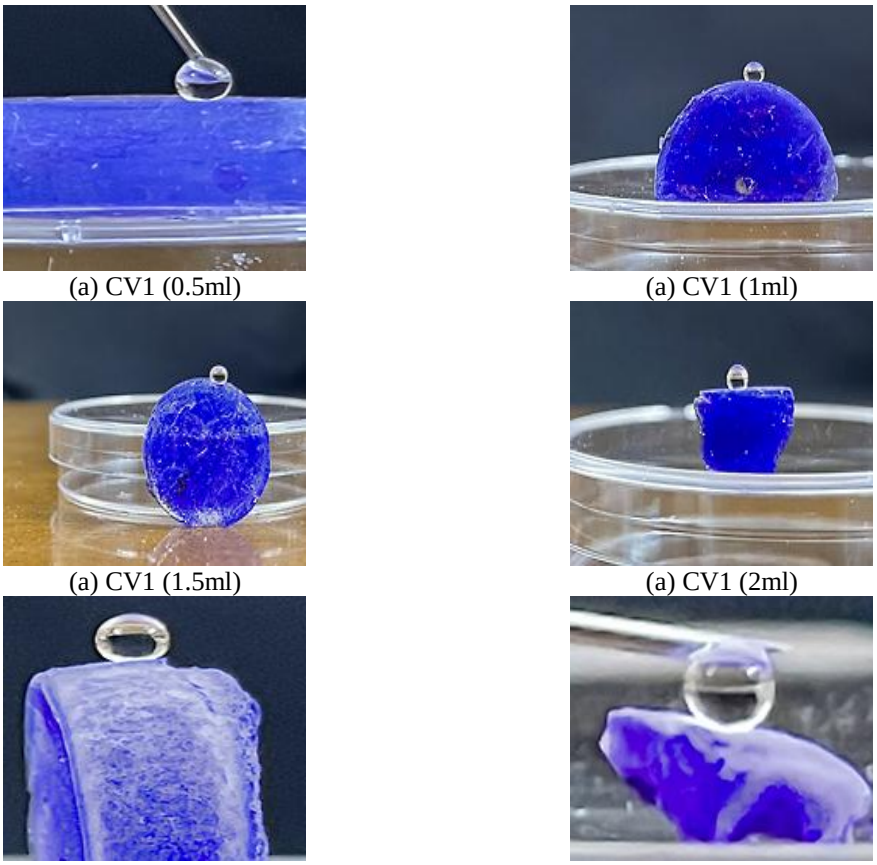

(a) CV1 (0.5ml) (a) CV1 (1ml)

(a) CV1 (1.5ml) (a) CV1 (2ml)

(a) CV2 (0.5ml) (a) CV2 (2 ml)

Fig. 6. Photographic image of doped silica aerogel prepared in different procedures

From Fig. 6, it can be said that the hydrophobicity property is affected by two parameters in this work; the first is the amount of dye, which means their concentration, and the second is the environment of preparation. Generally, it is observed that the dye concentration can improve the contact angle because of the nature of the structure of this dye, which consists of carbon and chloride molecules. Also, the pH of the sol was 8, which means that the preparation environment was basic. In alkaline solutions, nucleophilic hydroxyl ions attack the electrophilic central carbon of the dye, leading to the replacement of the hydroxyl ions with alkyl groups (Krause & Goldring, 2019).

4. Conclusions

The surface and composition properties of superhydrophobic silica aerogel are improved when doped with Crystal Violet dye under normal atmospheric pressure. In this work, n-hexane was used as the starting modifier for catalysis. This step played a significant role in retaining the dye within the silica network, leading to the attainment of a high contact angle, low density, and nano-homogeneous structure. This prompts us to think of increasing research and study in the future to use different types of laser dyes in grafting silica gel to obtain better specifications. and taking into account that the concentration has a significant role in changing the structural and spectral properties of the produced silica.

Acknowledgements

The authors would like to sincerely acknowledge, Ministry of High Education and Scientific Research, Mustansiriyah University. Also, many thanks to Ibin-Sina center of scientific examinations, Phi Nano-Science Center (PNSC), to help and supported.

References

Al-Sharuee, I.F. (2019). Thermal Conductivity Performance of Silica Aerogel after Exposition on Different Heating under Ambient Pressure. *Baghdad Science Journal, 16*(3 (Suppl.)), 0770-0770.

AL-Sharuee, I.F. (2021). Specifications study of Hydrophobic Silica Aerogel Doped with Rhodamine 6G Prepared via Sub-Critical Drying Technique. *Iraqi Journal of Science, 62*(2), 483-489.

Al-Sharuee, I.F., Mohammed, F.H. (2019). *Investigation study the ability of superhydrophobic silica to adsorb the Iraqi crude oil leaked in water.* Paper presented at the IOP Conference Series: Materials Science and Engineering.

Berardi, U., Zaidi, S.M. (2019). Characterization of commercial aerogel-enhanced blankets obtained with supercritical drying and of a new ambient pressure drying blanket. *Energy Buildings, 198*, 542-552.

Bhagat, S.D., Rao, A.V. (2006). Surface chemical modification of TEOS based silica aerogels synthesized by two step (acid–base) sol–gel process. *Applied Surface Science, 252*(12), 4289-4297.

Bi, C., Tang, G., & Transfer, M. (2013). Effective thermal conductivity of the solid backbone of aerogel. *International Journal of Heat, 64*, 452-456.

Błaszczyński, T., Ślosarczyk, A., & Morawski, M. (2013). Synthesis of silica aerogel by supercritical drying method. *Procedia Engineering, 57*, 200-206.

Cuce, E., Cuce, P.M., Wood, C.J., & Riffat, S.B. (2014). Toward aerogel based thermal superinsulation in buildings: a comprehensive review. *Renewable Sustainable Energy Reviews, 34*, 273-299.

Feng, G., Li, Z., Mi, L., Zheng, J., Feng, X., & Chen, W. (2018). Polypropylene/hydrophobic-silica-aerogel-composite separator induced enhanced safety and low polarization for lithium-ion batteries. *Journal of Power Sources, 376*, 177-183.

Gupta, P., Singh, B., Agrawal, A. K., & Maji, P. K. (2018). Low density and high strength nanofibrillated cellulose aerogel for thermal insulation application. *Materials Design, 158*, 224-236.

Han, X., Williamson, F., Bhaduri, G.A., Harvey, A., & Šiller, L. (2015). Synthesis and characterisation of ambient pressure dried composites of silica aerogel matrix and embedded nickel nanoparticles. *The Journal of Supercritical Fluids, 106*, 140-144.

Haque, F.Z., Husain, M. (2014). Synthesis and spectroscopic characterization of coumarin 440 dye doped silica gel rods. *Optik, 125*(10), 2308-2312.

He, S., Chen, X. (2017). Flexible silica aerogel based on methyltrimethoxysilane with improved mechanical property. *Journal of Non-Crystalline Solids, 463*, 6-11.

He, S., Huang, Y., Chen, G., Feng, M., Dai, H., Yuan, B., & Chen, X. (2019). Effect of heat treatment on hydrophobic silica aerogel. *Journal of Hazardous Materials, 362*, 294-302.

Hrubesh, L.W. (1998). Aerogel applications. *Journal of Non-Crystalline Solids, 225*, 335-342.

Karamikamkar, S., Naguib, H.E., & Park, C.B. (2020). Advances in precursor system for silica-based aerogel production toward improved mechanical properties, customized morphology, and multifunctionality: A review. *Advances in Colloid Interface Science, 276*, 1-29.

Kim, G.-S., & Hyun, S.-H. (2003). Synthesis of window glazing coated with silica aerogel films via ambient drying. *Journal of non-Crystalline Solids, 320*(1-3), 125-132.

Korppi-Tommola, J., Yip, R. (1981). Solvent effects on the visible absorption spectrum of crystal violet. *Canadian Journal of Chemistry, 59*(2), 191-194.

Krause, R.G., Goldring, J.D. (2019). Crystal violet stains proteins in SDS-PAGE gels and zymograms. *Analytical Biochemistry, 566*, 107-115.

Li, M., Jiang, H., Xu, D., Hai, O., & Zheng, W. (2016). Low density and hydrophobic silica aerogels dried under ambient pressure using a new co-precursor method. *Journal of Non-Crystalline Solids, 452*, 187-193.

Li, W.-C., Lu, A.-H., & Guo, S.-C. (2002). Control of mesoporous structure of aerogels derived from cresol–formaldehyde. *Journal of Colloid Interface Science, 254*(1), 153-157.

Li, X., He, H., Cui, S., & Ren, L. (2015). Synthesis and characterization of the monolithic NiO-Al2O3 aerogels. *ECS Journal of Solid State Science Technology, 5*(2), 1-3.

Linhares, T., de Amorim, M.T.P., & Durães, L. (2019). Silica aerogel composites with embedded fibres: a review on their preparation, properties and applications. *Journal of Materials Chemistry A, 7*(40), 22768-22802.

Liou, T.H. (2004). Preparation and characterization of nano-structured silica from rice husk. *Materials Science and Engineering: A, 364*(1-2), 313-323.

Mazrouei-Sebdani, Z., Begum, H., Schoenwald, S., Horoshenkov, K.V., & Malfait, W. (2021). A review on silica aerogel-based materials for acoustic applications. *Journal of Non-Crystalline Solids, 562*, 1-17.

Mohammed, M.T., & Hussein, S.M. (2020). Evaluation of structure and properties of various sol–gel nanocoatings on biomedical titanium surface. *Karbala International Journal of Modern Science, 6*(2), 215-224.

Nazriati, N., Setyawan, H., Affandi, S., Yuwana, M., & Winardi, S. (2014). Using bagasse ash as a silica source when preparing silica aerogels via ambient pressure drying. *Journal of Non-Crystalline Solids, 400*, 6-11.

Oh, K.W., Kim, D.K., & Kim, S.H. (2009). Ultra-porous flexible PET/Aerogel blanket for sound absorption and thermal insulation. *Fibers Polymers, 10*(5), 731-737.

Pan, Y., He, S., Gong, L., Cheng, X., Li, C., Li, Z., . . . Zhang, H. (2017). Low thermal-conductivity and high thermal stable silica aerogel based on MTMS/Water-glass co-precursor prepared by freeze drying. *Materials Design, 113*, 246-253.

Peterson, G.R., Hung-Low, F., Gumeci, C., Bassett, W.P., Korzeniewski, C., & Hope-Weeks, L. (2014). Preparation–Morphology–Performance Relationships in Cobalt Aerogels as Supercapacitors. *ACS Applied Materials Interfaces, 6*(3), 1796-1803.

Rao, A.V., Nilsen, E., & Einarsrud, M.-A. (2001). Effect of precursors, methylation agents and solvents on the physicochemical properties of silica aerogels prepared by atmospheric pressure drying method. *Journal of Non-Crystalline Solids, 296*(3), 165-171.

Sciuti, L., Gonçalves, T., Tomazio, N., de Camargo, A., Mendonça, C., & De Boni, L. (2019). Random laser action in dye-doped xerogel with inhomogeneous TiO 2 nanoparticles distribution. *Journal of Materials Science: Materials in Electronics, 30*(18), 16747-16754.

Shi, F., Wang, L., & Liu, J. (2006). Synthesis and characterization of silica aerogels by a novel fast ambient pressure drying process. *Materials Letters, 60*(29-30), 3718-3722.

Sinkó, K. (2010). Influence of chemical conditions on the nanoporous structure of silicate aerogels. *Materials, 3*(1), 704-740.

Štengl, V., Bakardjieva, S., Šubrt, J., & Szatmary, L. (2006). Titania aerogel prepared by low temperature supercritical drying. *Microporous Mesoporous Materials, 91*(1-3), 1-6.

Xie, T., He, Y.-L., & Hu, Z.-J. m. t. (2013). Theoretical study on thermal conductivities of silica aerogel composite insulating material. *International Journal of Heat, 58*(1-2), 540-552.

Xu, J., Jia, P., Wang, X., Xie, Z., Chen, Z., & Jiang, H. (2021). The aminosilane functionalization of cellulose nanocrystal aerogel via vapor-phase reaction and its CO2 adsorption characteristics. *Journal of Applied Polymer Science, 138*(35), 1-12.

Yaghoobi, H., Fereidoon, A. (2018). Modeling and optimization of tensile strength and modulus of polypropylene/kenaf fiber biocomposites using Box–Behnken response surface method. *Polymer Composites, 39*, 463-479.

Yuan, B., Ding, S., Wang, D., Wang, G., & Li, H. (2012). Heat insulation properties of silica aerogel/glass fiber composites fabricated by press forming. *Materials Letters, 75*, 204-206.

Yun, S., Luo, H., & Gao, Y. (2014). Superhydrophobic silica aerogel microspheres from methyltrimethoxysilane: rapid synthesis via ambient pressure drying and excellent absorption properties. *RSC Advances, 4*(9), 4535-4542.